JOURNAL OF GEOPHYSICAL RESEARCH, VOL. 113, G03S06, doi:10.1029/2008JG000682, 2008

Simulating nonsorted circle development in arctic tundra ecosystems

Ronald P. Daanen,[1] Debasmita Misra,[2] Howard Epstein,[3]
Donald Walker,[4] and Vladimir Romanovsky[1]

Received 2 January 2008; revised 1 April 2008; accepted 15 April 2008; published 15 July 2008.

[1] Nonsorted circles, ubiquitous to the Arctic Tundra region, are patterned ground features with circular semibarren areas surrounded by vegetation. These circles are formed and persist as an ecosystem due to complex soil-water-energy-ice-plant relationships and dynamics in the Arctic. In this paper, we present the first model that captures the dynamics of the physical and biological components of the nonsorted circle ecosystem in order to understand its formation and persistence, especially in a changing climatic environment. We have applied a coupled model describing (1) vegetation dynamics (ArcVeg) and (2) coupled heat and moisture transport with phase change (WIT) in the active layer of the soil where such circles are initiated and developed. We simulated the system behavior during the formation process starting with a random vegetation development. The vegetation provided heterogeneous insulation to the soil surface. During freezing, the noninsulated areas froze first, resulting in preferential ice accumulation in those areas. The ice prevented the vegetation from developing further in those areas and thus developed and stabilized the nonsorted circle pattern. The model produced a nonsorted circle pattern that was well compared to those observed in the field. The model also illustrated that the availability of water was critical for the sustenance and stability of the nonsorted circle. The effect of climatic variations on the freezing process on the other hand did not seem to affect the formation and sustenance of nonsorted circles.

Citation: Daanen, R. P., D. Misra, H. Epstein, D. Walker, and V. Romanovsky (2008), Simulating nonsorted circle development in arctic tundra ecosystems, *J. Geophys. Res.*, *113*, G03S06, doi:10.1029/2008JG000682.

1. Introduction

[2] The interdependency of biological and physical components of the arctic tundra system can yield strongly nonlinear processes with potential thresholds for ecosystem shifts. The nonsorted circle ecosystem is an example of this type of complex system for which the driving forces are poorly understood. Nonsorted circles are a form of patterned ground with areas of heaves and troughs, ubiquitous to the arctic tundra, that result from cryoturbation [*Vliet-Lanoe*, 1991] (Figure 1). From a physical perspective, hydrology plays an important role in ecosystem dynamics in the nonsorted circles. Even though the tundra appears to have a relatively simple hydrologic system, often consisting of only a saturated active layer (the surface soil layer that thaws on an annual basis) underlain by permafrost, the impact of hydrology on maintaining the equilibrium of the nonsorted circle ecosystem is significant. Disturbances associated with the freezing and thawing of the active layer (i.e., cryoturbation) are key hydrological processes that interact with the biological component of the system and shape the arctic tundra [*Vliet-Lanoe*, 1991].

[3] Nonsorted circles (sometimes referred to as frost boils or mud boils) are a patterned-ground feature of approximately 1–3 m in diameter. These features generally have little or no vegetation on them due to excessive soil expansion from ice accumulation during winter [*Washburn*, 1956]. Nonsorted circles are, however, typically surrounded by dense vegetation, which acts as an insulator against fall cooling, leading to preferential formation of ice within the less-vegetated circles. The water needed for the observed ice formation within the circle (heaving areas) migrates horizontally from vegetation-covered soils (trough areas), peripherally from outside the circle, as a result of increased tension (capillary pressure) within the circle during freezing [*Daanen et al.*, 2007; *Ippisch*, 2003]. Thus, moisture migrates laterally due to horizontal differences in insulation at the soil surface. The nonsorted circle system is defined as an area within the arctic tundra with at least one nonsorted circle and its peripherally surrounding tundra (Figure 1).

[4] Water is generally abundant in the southern arctic tundra during fall freezing. The abundance of water in the active layer may partly be a product of snowmelt and thawing soil over the spring and summer and a part of it might originate from increased late summer or fall precip-

[1]Permafrost Laboratory, Geophysical Institute, University of Alaska Fairbanks, Fairbanks, Alaska, USA.
[2]Department of Mining and Geological Engineering, College of Engineering and Mines, University of Alaska Fairbanks, Fairbanks, Alaska, USA.
[3]Department of Environmental Sciences, University of Virginia, Charlottesville, Virginia, USA.
[4]Department of Biology and Wildlife, University of Alaska Fairbanks, Fairbanks, Alaska, USA.

0148-0227/08/2008JG000682$09.00

Figure 1. Individual nonsorted circles in the top part of the figure and an aerial view of patterned ground with ice wedge polygons and nonsorted circles in the bottom half of the figure.

itation combined with reduced evaporation. The permafrost below the active layer prevents any vertical drainage, thus creating the potential for inundated soils. Nonsorted circles tend to form in areas that are mostly flat so little water tends to drain laterally. Abundance of water and the texture of the soil are the major drivers of frost heave (the process of soil expansion as a result of ice lens formation during freezing), which results in formation of patterned ground features such as the nonsorted circles [*Vliet-Lanoe*, 1985]. In general, fine-textured soils with relatively high hydraulic conductivities, like silts, are susceptible to frost heave [*Mitchell*, 1993]. Cryoturbation (movement of soil) due to frost heave prevents vegetation growth and succession in ice accumulation areas.

[5] The presence of vegetation and organic matter in certain areas (trough regions) of the nonsorted circle ecosystem restricts heat flow into and out of the ground by offering insulation. Surface heat fluxes combined with the movement of water in the soil determine the strength and location of ice accumulation and cryoturbation. It is observed within the nonsorted circle system that areas with little vegetation (less surface insulation) experience more frost heave during the winter than areas with dense vegetation cover [*Walker et al.*, 2008].

[6] An estimate of the insulation properties of the soil surface is expressed with an R-value. The R-value is related to the thickness of the insulative layer and the inverse of its thermal conductivity. It is commonly used in cold region construction engineering to express insulation efficiency. The areas with little vegetation, organic matter and snow cool faster in the fall and thus have lower R-values compared to areas with abundance of these. Snow accumulation across tundra landscapes tends to be slightly greater at lower slope positions, and snow accumulates preferentially in vegetated areas where it can be trapped [*Sturm et al.*, 2005]. Presence or absence of such insulation affects the position and dimension of the nonsorted circles in the arctic tundra. The detailed processes governing the formation and persistence of nonsorted circles and their effects on soil-plant-water relationships are still being studied. In this paper, we have attempted to gain understanding of such processes and relationships using a numerical modeling exercise with some knowledge of the physical and biological processes and their interplay.

[7] Several modeling studies have focused on ice lens formation leading to substantial soil expansion (frost heave) [*Miller*, 1980; *Fowler and Krantz*, 1994]. Several of these models have been developed for only a single dimension which is insufficient to capture the hydrological dynamics of a nonsorted circle system [*Boike et al.*, 2002]. *Nicolsky et al.* [2004] developed a two-dimensional model that accurately estimates frost heave for a single nonsorted circle, assuming an open system with an unlimited supply of water. However, even in a relatively saturated arctic tundra system, the available water is limited; therefore for accurate results, the supply of water initiating frost heave must be accounted for within the domain of simulation. *Ippisch* [2003] developed a three-dimensional model that also captures the dynamics of a single nonsorted circle. However, the model focus is more on gas and solute flow than on the dynamics of liquid water and ice. The modeling of these systems could be improved to include coupled biological and physical processes across a domain larger than just a single nonsorted circle. Our hypothesis is that the interplay between the physical and the biological processes of the system, which are affected by changes in the climatic, environmental and soil properties, govern the initiation, development, and sustenance of nonsorted circles.

[8] Climate models predict dramatic changes for the arctic tundra environment, such as shifts in summer and winter temperatures, with enhanced winter precipitation [*Maxwell*, 1992; *Walsh*, 1993]. Ecosystem changes caused by recent climate warming are becoming apparent in the arctic tundra [*Chapin et al.*, 2005; *Jia et al.*, 2003; *Myneni et al.*, 1997; *Tape et al.*, 2006; *Walker et al.*, 2006], and the effect of changing ecosystems on patterned-ground features such as the nonsorted circle ecosystem and subsequent system feedbacks are areas of active contemporary research [*Walker et al.*, 2004]. Climate warming has been shown to change arctic vegetation quantity and composition [*Jia et al.*, 2003; *Walker et al.*, 2006], thus affecting local and regional energy budgets, and hydrological processes [*Chapin et al.*, 2005]. Understanding the active layer hydrology and its relationship with soils and plants in the arctic tundra (Figure 1) will help us in the future to assess the impact of climate warming and the subsequent effect on ecosystems, such as the nonsorted circles, in cold regions of the Earth.

[9] The objective of this study is to identify the sensitivity of active layer, surface, and atmospheric properties on the spatial pattern and size and thus the effect on the equilib-

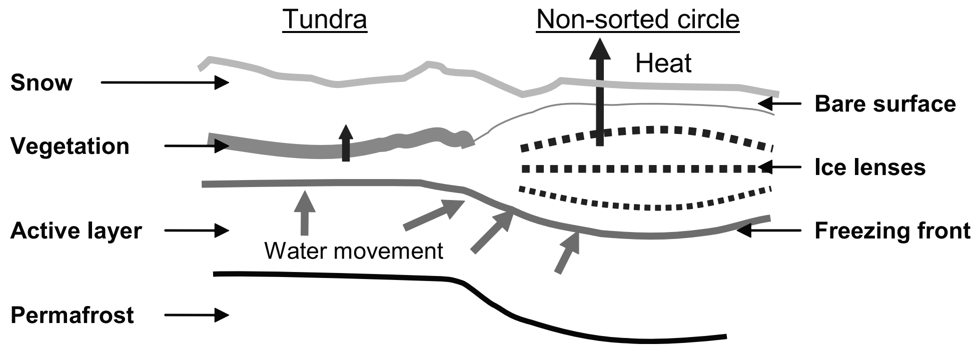

Figure 2. A conceptual diagram of the heat and water fluxes in the active layer of the nonsorted circle ecosystem.

rium of the nonsorted circle ecosystem using the coupled WIT-ArcVeg model.

[10] Figure 2 is a conceptual model that illustrates the importance of hydrology in maintaining the local balance of physical, chemical and biological processes in the nonsorted circle ecosystem. In a simplified representation of the system, we consider ice accumulation caused by temperature gradients, which result from differences in insulation (by vegetation, organic matter, snow) at and near the soil surface. The physics of this simplified system is represented in a Water Ice Temperature (WIT) model [*Daanen*, 2004; *Daanen et al.*, 2007], and the biological aspects (i.e., vegetation and organic matter) are simulated using the ArcVeg model [*Epstein et al.*, 2000].

2. Methods

2.1. WIT

[11] WIT (Water Ice Temperature) is a three-dimensional model that simulates coupled heat and moisture transfer [*Daanen et al.*, 2007]. The model is based on the Richard's equation (unsaturated porous media water mass balance and mass transfer equation) and Fourier's law transient equation for energy conservation and heat conduction) with phase change and convective heat flux. Phase change is regulated by the generalized Clapeyron equation and the freezing characteristics curve of the soil. The model was originally developed to simulate heat and water flow in snow (R. P. Daanen and J. L. Nieber, Liquid water model for snow, submitted to *Journal of Cold Regions Engineering*, 2007). The horizontal movement of water through soils as a result of temperature gradients during freezing has been investigated with the WIT model [*Daanen et al.*, 2007]. WIT simulates water movement in the active layer and ice accumulation as a result of differential surface insulation.

[12] The boundary conditions can be specified as fluxes for heat and water (Neumann condition) or as Dirichlet boundaries of specified temperature and pressure. A third order boundary condition is applied at the upper and lower boundary, where the permafrost boundary temperature and the air temperature affect the freezing rate of the active layer. Table 1 gives a summary of the input for the WIT model. For the calibration and validation of the WIT model we refer the readers to *Daanen et al.* [2007].

2.2. ArcVeg

[13] The arctic vegetation dynamics model (ArcVeg) [*Epstein et al.*, 2000, 2001] is used to simulate vegetation development, a key component of the upper boundary description. The ArcVeg model controls the dynamics of the surface insulation by simulating vegetation succession on small patches of tundra. ArcVeg simulates vegetation growth as expressed by a variety of different plant functional types, including grasses, sedges, mosses, lichens, forbs, evergreen and deciduous shrubs. Each plant type has its own germination probability, and each year new seeds can germinate and either initiate or contribute to the biomass of that plant type. Composition of plant functional types is also affected by competition among types for plant-available nitrogen in the soil. Each plant functional type has its own sensitivity to the climate (i.e., temperature in this case), and therefore the composition of the vegetation

Table 1. Model Input Data Summary

Model	Soil Physics	Air Temperature	Permafrost Temperature	Climate	Plant Growth	Nitrogen Dynamics
WIT	Sand, Silt, Clay, Moisture content	High arctic, Franklin Bluffs, Low arctic	$-1.0°C$ at 1.7 m depth	Determines air temperature	Converts to insulation	
ArcVeg		Determines bioclimatic zone	Determines bioclimatic zone	Bioclimatic zone A-E from the high arctic to the low arctic	Seed germination, Senescing, Biomass production	Plant type competition, Soil organic nitrogen

changes depending on the climatic conditions. The model stochastically generates climate disturbance and grazing. The patches disturbed by frost heave experience a negative effect due to increased mortality of the vegetation. Table 1 gives a summary of the input variables for the ArcVeg model.

[14] ArcVeg is a stochastic model which solves plant biomass accumulation based on soil nutrition and plant competition with a Monte Carlo approach. The model simulates climate variations for each of the five arctic tundra subzones (http://www.geobotany.uaf.edu/cavm/). ArcVeg was developed for the southern portion of the arctic tundra and adapted for other bioclimatic subzones further north [*Walker et al.*, 2008]. Because plant-available nitrogen can be a strongly limiting nutrient for tundra plants [*Shaver et al.*, 2001], the model functions essentially with nitrogen mass balance, moving nitrogen among soil organic matter, soil inorganic nitrogen, and plant pools. The plant parameters include nitrogen uptake efficiencies, the biomass:N ratio, annual proportion of plant material senescing, probability of seedling establishment, and cold tolerance for growth. The model runs on an annual time step, but the growing season is split into five distinct plant-growth periods (the first period follows the onset of growth after the spring thaw, and the last growth period includes the peak of the growing season through senescence), to capture the seasonality of growth. For the calibration and validation of the ArcVeg model we recommend readers to review *Epstein et al.* [2001, 2000] and *Walker et al.* [2008].

2.3. Coupled Models

[15] WIT and ArcVeg are coupled dynamically in three ways; (1) ice accumulation (either ice lenses or needle ice) in a soil column yields an increased amount of vegetation mortality in that node, due to root damage [*Jonasson and Callaghan*, 1992]: this ice accumulation is assessed after each freezing calculation; (2) vegetation biomass provides insulation, expressed as an R-value, which determines the upper boundary temperature of the WIT model, the insulation is calculated after multiple years of vegetation development in which the ice accumulation pattern is kept constant. The number of years of vegetation development between freezing calculations is stepped up according to the following equation: $years = frnum + (frnum - 1) \times 3$, where *frnum* is the number of freezing periods previously simulated. The insulation is calculated using a simple linear relation between individual plant biomass and insulation. The equation is as follows,

$$\begin{aligned} &\text{if}\ \overline{biomass}^{i} < 1 \\ &R = \frac{\left(\sum biomass^{i,j} \times c^{j}\right) \times 3}{1} \\ &\text{else} \\ &R = \frac{\left(\sum biomass^{i,j} \times c^{j}\right) \times 3}{1/\overline{biomass}^{i}} \end{aligned} \qquad (1)$$

where $\overline{biomass}^{i}$ is the average biomass in the ith plot, $biomass^{i,j}$ is from the ith plot and jth plant type, c^j is a constant for each plant type to relate it to insulation for the simulation. In this paper we have used 0.1 (c^j) for all plant types except for moss where we used 50 (c^j), the constant 3 is to correct for snow cover. (3) Soil organic matter calculated by ArcVeg affects the freezing characteristic and hydraulic conductivity curves for the soils in WIT. Higher soil organic matter leads to an increase in the freezing point depression and an increase in the hydraulic conductivity. These changes are made by linearly adjusting the ‘n’ parameter in the Van Genuchten [*van Genuchten*, 1980] equations for the freezing characteristic curve and unsaturated hydraulic conductivity curve (see *Daanen et al.* [2007] for description of van Genuchten parameters and freezing characteristic curve). As ArcVeg simulates vegetation production during each growing season, warmer years lead to greater productivity and plant community development than colder years. Annual frost heave on patches that have minimal insulation from vegetation inhibits vegetation from colonizing these areas. Disturbed patches therefore tend to persist on the landscape due to disturbance feedbacks associated with frost heave and vegetation. The model is typically allowed to run until an equilibrium vegetation community is established. Figure 4 shows the patterns generated by WIT-ArcVeg with a model run of 861 years. For our simulations, we parameterized the effect of ice on the vegetation and the effect of vegetation on the heat flux so that they interacted to produce a pattern.

[16] Pattern formation due to differential cooling of the active layer was simulated using the combined models WIT-ArcVeg. Our reference run was for conditions equivalent to those found near Franklin Bluffs on the North Slope of Alaska, and we found a good match between predicted and observed number of nonsorted circles per unit area [*Raynolds et al.*, 2008]. We then varied the following parameters in WIT: soil moisture, soil texture, active layer depth, and air temperature. The variables used by the ArcVeg model were kept constant. Table 1 gives an overview of the input variables of both models.

2.4. R-Values

[17] We used a simplified relation between plant biomass and insulation in our model. To justify this relationship we used field measurements of biomass and temperatures of the same plant communities. Air temperatures, soil temperatures just below the vegetation and organic layer, and the temperature of the permafrost at 1 m depth were measured and logged continuously in the field in 2004 and 2005 [*Kade et al.*, 2006]. In this study we used the R-value to evaluate the insulation capacity of the land surface (i.e., a combination of the effects of vegetation, organic matter, snow) using these temperature records, for both nonsorted circles and undisturbed tundra. Using simple heat conduction principles in completely frozen soil we determined the heat flux between the mineral soil surface and the permafrost. We used an estimate for the thermal conductivity and depth of the soil surface layer and the soil heat flux to calculate the mineral soil surface temperature, by assuming the soil surface heat flux to be the same as the deeper heat flux calculated previously. The R-value of the soil surface was calibrated by matching calculated mineral soil surface temperatures with the observed. Vegetation, dead organic matter, and snow were all included to produce an aggregate R-value for each site.

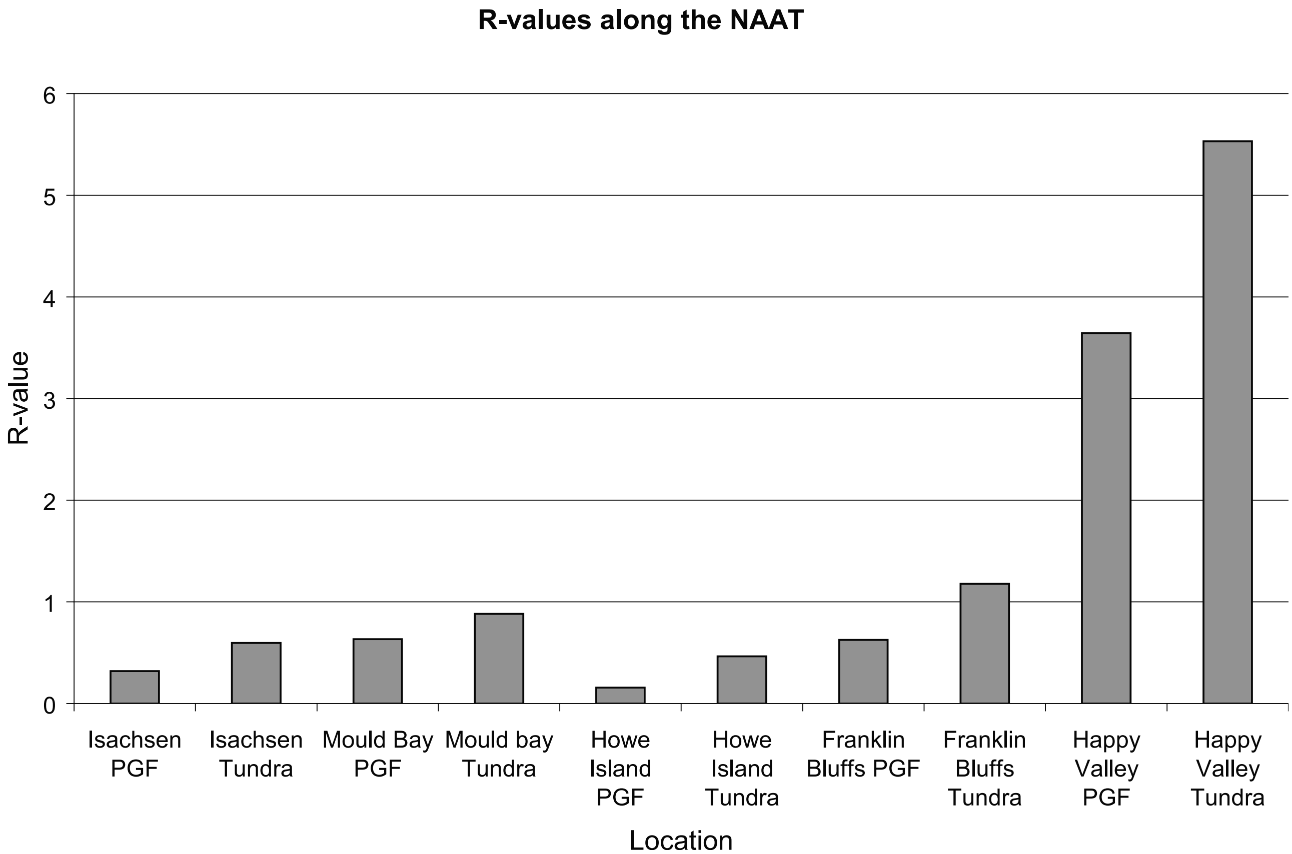

Figure 3. Summary of the average R-values for selected sites along the NAAT (from left to right are the cooler to warmer locations).

[18] We used a multiple linear regression analysis on observed biomass data from the North American Arctic Transect (NAAT) [*Walker et al.*, 2008] to determine how well plant biomass predicted these calculated R-values. Biomass data from 7 different plant types were used along with the end of season snow depth to predict the measured R-value.

3. Results

[19] R-values increased, as expected from north to south along the NAAT, with an increase in vegetation, dead organic matter, and snow depth (Figure 3). From the observed data over the entire north to south transect there appears to be a positive relationship between the surface live vegetation biomass (over all plant types) and the R-value, but there is a lot of variability in this relationship. Part of this variability is caused by plant species-specific insulation to the soil surface. Moss tends to have a greater effect on the insulation than graminoids, for example. Also, the problem could be compounded by preferential snow accumulation under or near particular plant species. Predicting the insulation from observed living biomass using seven plant types and snow depth in a multiple linear regression method over the entire gradient is possible with an r-square value of 0.82. In Table 2, we present the different biomass and snow depth values with the resulting multiple linear regression prediction according to the following equation,

$$R = -0.38 + 0.056 * A - 0.0003 * B - 0.00007 * C - 0.156 * D - 0.0005 * E + 0.0038 * F - 0.0016 * G + 0.002 * H \qquad (2)$$

where R is the R-value, A is cm of snow, B is biomass (g/m^2) of deciduous shrubs, C is biomass (g/m^2) of evergreen shrubs, D is biomass (g/m^2) of horsetail, E is biomass (g/m^2) of lichen, F is biomass (g/m^2) of graminoids, G is biomass (g/m^2) of other forbs and H is biomass (g/m^2) of mosses. The end of season maximum snow depth shows the strongest individual positive correlation in predicting the insulation value during the freezing period. Horsetail is the strongest negative predictor for R-value; this is likely related to increased soil moisture and maybe convective heat flow in horsetail habitat. Beside the direct effects of the plants on insulation, there may also be an effect of the plants on snow accumulation, although that correlation was low in this data set.

[20] We used WIT-ArcVeg to simulate the formation of a nonsorted circle system using a homogeneous soil domain and a random plant seeding. The results of these simulations are expressed in vegetation distributions (Figures 4 and 5). Figure 4 illustrates the development of a nonsorted circle system. Green colors represent greater plant biomass and

Table 2. Zonal Biomass Distribution Over the NAAT Over Seven Different Plant Types With the Prediction of the R-Value From Those Seven Different Plant Types and Snow Depth (R^2 = 0.82)

Location	Site Id.	Snow (cm)	Deciduous Shrubs (g/m^2)	Evergreen Shrubs (g/m^2)	Horsetail (g/m^2)	Lichens (g/m^2)	Graminoids (g/m^2)	Other Forbs (g/m^2)	Mosses (g/m^2)	Total Biomass (g/m^2)	R Value	Pred. R
Happy Valley nonfeature	HVRV066	77	299.5	168.63	0	12.59	217.71	0.58	263.9	1208.54	4.38	5.21
69°08 N	HVRV084	71	59.54	331.71	0	34.14	159.35	22.77	282.89	1293.11	7	4.70
148°51W	HVRV085	65	68.62	88.06	0	144.86	7.92	1.42	202.1	666.04	5	3.62
	HVRV087	73	111.52	253.9	0	13.63	165.39	59.81	143.99	1075.14	4.4	4.49
	HVRV086	77	184.63	151.37	0	11.69	197.44	4.78	116.19	894.47	6.88	4.85
Happy Valley feature	HVRV094	55	0	124.15	0	80.17	177.17	6.2	144.77	711.61	5	3.62
	HVRV083	67	22.56	81.61	0	126.5	31.32	6.3	253.05	669.95	4.38	3.94
	HVRV093	60	67.68	307.1	0	162.92	149.96	11.92	49.24	1115.92	2.5	3.52
	HVRV095	70	32.72	194.79	0	192.45	71.26	38.17	132.69	926.87	5	3.92
	HVRV053	66	109.36	0	0	14.28	3.32	0	10.24	203.2	3.13	3.32
	HVRV054	63	0	0.84	0	28.8	5	0	0	98.48	3.13	3.16
	HVRV056	64	0	0	0	0	0.2	0	0	64.2	3.5	3.21
	HVRV082	55	0	243.31	0.1	143.5	95.07	6.65	101.59	888.53	2.5	3.16
Franklin Bluffs nonfeature	FBRV011	21	58.6	202.81	6.06	31.29	61.4	20.94	257.45	862.36	0.4	0.54
69°40 N	FBRV012	32	84.69	296.45	1.52	36.7	55.49	23.81	127.93	955.04	1	1.56
148°44W	FBRV034	28	30.99	303.15	8.24	81.98	24.92	6.8	327.77	1115	0.7	0.60
	FBRV035	14	72.57	243.97	1.43	68.22	60.63	52.51	163.44	920.74	0.8	0.60
	FBRV018	57	36.34	223.32	0	0.01	120.87	0	59.11	719.97	1.2	3.37
	FBRV019	34	35.01	209.81	4.09	23.75	175.68	13.21	161.76	867.12	1.6	1.83
	FBRV020	33	45.71	246.52	1.52	8.78	183.62	10.22	66.74	842.63	1.6	2.02
	FBRV046	36	298.54	39.56	0	0.43	83.46	13.55	47.29	558.39	1.3	1.95
	FBRV047	41	14.21	59.72	1.3	13.11	168.09	0.49	49.58	407.22	2	2.44
Franklin Bluffs feature	FBRV006	7	6.93	5.96	0.93	2.66	14	65.11	1.61	110.16	0.125	−0.18
	FBRV009	10	0	0	0.26	1.01	2.59	20.03	3.79	37.88	0.4	0.13
	FBRV010	10	0	0	1.44	15.27	5.28	40.85	0	72.84	0.4	−0.09
	FBRV031	8	0	0.26	0	0	2.65	10.9	0	22.07	0.35	0.06
	FBRV033	10	0	0.16	0	4.25	0.74	31.27	1.16	47.74	0.18	0.14
	FBRV005	14	13.85	88.01	0	94.62	13.93	121.38	61.25	496.35	0.24	0.34
	FBRV007	30	1.46	99.76	5.53	213.63	16.07	74.31	11.41	556.99	0.45	0.30
	FBRV008	11	29.33	143.49	0	96.15	39.67	31.99	82.77	578.04	0.4	0.45
	FBRV030	20	39.48	64.12	0	77.96	17.22	68.02	16.7	367.62	0.25	0.69
	FBRV032	6	0	41.97	0	112.95	48.68	69.92	7.68	329.17	0.38	−0.01
	FBRV096	21	0	178.84	0	93.33	60.94	26.72	26.33	586	0.5	0.99
	FBRV097	18	0	146.94	3.02	173.48	68.12	18.07	29.2	605.83	0.45	0.35
	FBRV140	29	3.43	144.35	0	70.43	48.02	28.79	155.26	625.33	0.5	1.66
	FBRV001	37	0	0	4.39	0	34.63	2.86	0.51	79.39	1.5	1.14
	FBRV002	35	0	0	0.6	0	6.64	0	0	42.24	1.5	1.52
	FBRV004	57	0.6	0	1.03	0.56	88	6.66	3.5	157.35	2	2.99
	FBRV036	19	1.64	125.89	0.14	58.05	34.83	109.26	11.66	486.51	1	0.62
Howe Island nonfeature	HIRV022	13	221.09	530.77	0	0.3	1.49	1.99	94.38	1393.79	0.5	0.45
70°18 N	HIRV027	7	298.79	103.76	0	0	1.12	3.77	42.75	563.99	0.625	0.02
147°56W	HIRV028	22	276.14	647.02	0	0.2	1.32	22.53	113.28	1729.51	0.4	0.94
	HIRV116	8	21.21	371.02	0	1.57	1.99	13.44	53.21	842.49	0.4	0.14
	HIRV112	7	14.33	1070.05	0	2.16	0	0	133.58	2297.17	0.4	0.21
Howe Island feature	HIRV021	5	0	0	0	0	0.03	0	0	5.03	0.16	−0.10
	HIRV024	18	0	0.62	0	0	0.34	0	0	19.58	0.2	0.63
	HIRV110	7	0	0	0	0	0	0	0	7	0.13	0.02
	HIRV113	5	0	0	0	0	2.91	2.56	0	10.47	0.13	−0.09
	HIRV114	7	0	0	0	0	1.6	0.14	0	8.74	0.16	0.02
Mould bay nonfeature	MBRV411	21	54.83	51.19	0	8.66	0.16	5.64	126.57	319.24	1	1.03
76°14 N	MBRV404	10	0	0	0	1.37	3.97	9.53	244.67	269.54	0.7	0.69
119°19W	MBRV407	10	78.78	0	0	1.44	12.77	0	73.91	176.9	0.7	0.36
	MBRV409	21	44.01	0	0	7.03	0.87	121.43	96.8	291.14	0.9	0.80
	MBRV413	24	30.24	8.63	0	39.51	1.07	10.61	291.82	414.51	1	1.53
	MBRV415	27	1.17	0	0	36.75	9.34	20.44	331.49	426.19	1	1.81
Mould Bay feature	MBRV403	0	0	0	0	34.28	2.57	7.34	16.34	60.53	0.4	−0.36
	MBRV410	16	0.03	0	0	24.89	1.38	3.83	2.93	49.06	0.8	0.51
	MBRV412	14	0.15	0	0	46.7	5.38	35.92	2.03	104.18	0.7	0.35
Isachsen nonfeature	ISRV510	40	0	0	0	110	26	15	183.19	374.19	1	2.27
78°47 N	ISRV514	27	0	0	0	144	12	89	123.1	395.1	0.7	1.23
103°32W	ISRV518	20	0	0	0	173.6	44	72	148.09	457.69	0.75	1.02

Table 2. (continued)

Location	Site Id.	Snow (cm)	Deciduous Shrubs (g/m^2)	Evergreen Shrubs (g/m^2)	Horsetail (g/m^2)	Lichens (g/m^2)	Graminoids (g/m^2)	Other Forbs (g/m^2)	Mosses (g/m^2)	Total Biomass (g/m^2)	R Value	Pred. R
	ISRV520	11	0	0	0	88.6	12.6	47.7	116.9	276.8	0.2	0.41
	ISRV516	11	0	0	0	209	29	85	182.35	516.35	0.33	0.49
Isachsen feature	ISRV521	32	0	0	0	32	0	2	16	82	0.3	1.43
	ISRV501	5	0	0	0	0.3	7.6	5	0	17.9	0.25	−0.08
	ISRV504	2	0	0	0	0	1.84	2.2	0	6.04	0.6	−0.26
	ISRV505	14	0	0	0	0	3.9	1.6	0	19.5	0.11	0.42
	ISRV506	5	0	0	0	0	3.9	0	0	8.9	0.25	−0.08
	ISRV507	0	0	0	0	0	11.8	0	0	11.8	0.17	−0.33
	ISRV511	15	0	0	0	3	5	14	3	40	0.33	0.47
	ISRV515	15	0	0	0	0	2	9	0	26	0.33	0.46
	ISRV517	23	0	0	0	0.1	2.9	1.4	16	43.4	0.25	0.95
	ISRV519	13	0	0	0	108	2.5	5	51	179.5	0.6	0.41

the gray and white tones represent lower plant biomass. The simulation started with random seeding of plants and was stopped after 20 freezing cycles or 861 years of plant biomass development demonstrating the formation and sustenance of a nonsorted circle. The time steps and conditions used in our simulation demonstrated a distinct pattern of nonsorted circles as output on the year 861 after inception. Although, we have no way to validate the time period required for a distinct pattern development of the nonsorted circles, our simulation provides an understanding of this time period for specific conditions used.

[21] Sensitivity of active layer properties and climate is also presented as vegetation distributions obtained from the WIT-ArcVeg model. Parameters such as the soil moisture, the soil texture and the active layer depth caused a change in the pattern formation. However, a variation in the air temperature seem to have no effect on the pattern formation. The central illustration in Figure 5 is the reference run with selected input parameters for soil, water content and active layer depth from the Franklin Bluffs research site. The distribution in the reference run is similar to the distribution found in field. Soil moisture had a strong effect on pattern formation and nonsorted circle development. Cold and moderate arctic air temperatures yielded a similar number and size of nonsorted circles. The active layer depth had a strong influence on the number and size of the nonsorted circles that developed, with shallower active layers prohibiting the formation of circles. Reducing the active layer depth from 70 cm to 60 cm, completely eliminated the nonsorted circle features. Soil texture played an important role, as it determined the freezing characteristics curve and the hydraulic conductivity. The patterns are strongly affected by the texture of the soil with no nonsorted circles being formed in the sandy soil (coarse texture) and a large number of smaller nonsorted circles being formed in the clayey soil (fine texture), compared to the silty soils of Franklin Bluffs.

4. Discussion

[22] The R-values used in this study are calculated based on heat conduction principles. This means that other sources of heat, such as radiation and convection by air at or near the soil surface are not included in the analysis. During the summer months those additional sources of energy should not be ignored. However, during the snow covered, frozen season those heat sources are assumed to be negligible.

[23] Plant biomass is not related to snow depth along the NAAT [*Kade et al.*, 2006]. However, the snow depth used to determine the relationship between plant biomass and snow depth in that study was the end of season snow depth. This deep snowpack is less likely to be correlated with the smaller vegetation found in the tundra. Early season snow depth may have a better correlation with vegetation due to trapping of the snow, however we lack the data to support this hypothesis. The observation we made for the R-value are comparable to what is generally expected, i.e., further north and on disturbed locations the R-value declined due to weaker plant growth conditions [*Walker et al.*, 2008]. This simplified relation between plant biomass and insulation was used to couple ArcVeg to WIT and calculate the insulation at the soil surface.

[24] Patterns in the arctic tundra have been studied over the last century [*Washburn*, 1997]. Many initiation processes are proposed to explain the formation of the multitude of patterned ground features [*Washburn*, 1956]. *Peterson and Krantz* [2003] described an initiation process for nonsorted circles. They used linear stability analysis on the physical description of freezing front movement to identify the most likely spacing between features: that study did not show the dynamics of the system. In this study we have used WIT in conjunction with ArcVeg to generate patterns from initially random vegetation development. We conclude that the soil and vegetation characteristics determine the spacing and size of the features [*Daanen et al.*, 2007]. The fairly simple approach of coupling stochastic and physical processes can yield complexity that shapes the pattern of the system. We show with our modeling approach that the hydrological component is important for vegetation survival in the ecosystem through its mobility from insulated to noninsulated areas during freezing, which prevents root destruction by ice lens formation.

[25] We found that the degree of wetness of the soil is an important variable for nonsorted circle pattern formation. Lack of water in the soil can completely prevent the formation of patterns due to the absence of ice formation in the soil. The tundra is however mostly saturated because of the permafrost boundary underneath the active layer that prevents drainage. With change in climate, especially during dry years or due to improved drainage with deeper active

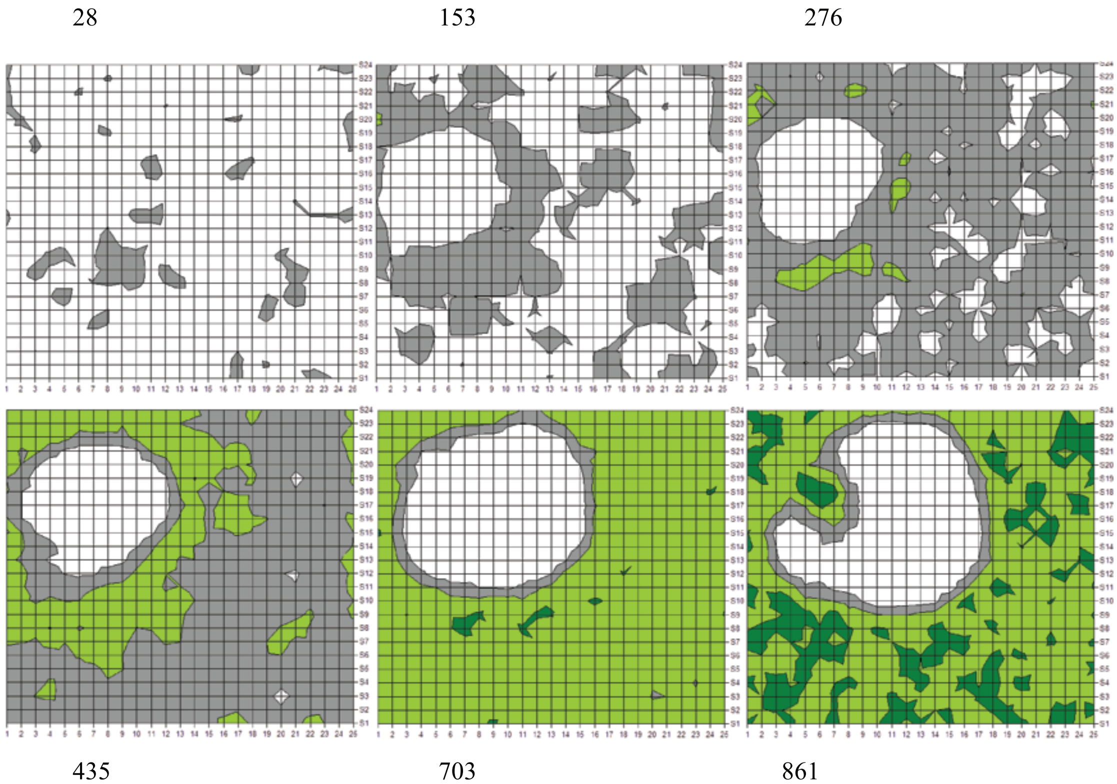

Figure 4. Initiation, development, and formation of a single nonsorted circle using Wit-ArcVeg coupled model. Color indicates vegetation density with dark green the highest and white the lowest vegetation density. Each grid square is 10 × 10 cm and the total domain is 2.5 × 2.5 m. The numbers on top and the bottom indicate the number of years the vegetation was developing.

layers [*Hinzman et al.*, 2005], some of the barren areas (nonsorted circles) could become vegetated due to lack of ice accumulation thus changing the equilibrium of the physical processes.

[26] The effect of air temperature variations during freezing on feature formation is very small in our comparison. For the modeling we used the measured air temperature from colder and warmer regions along the NAAT and the results show little difference between warmer or colder climate conditions on the physical behavior of the freezing process. This means that the freezing process or cooling rate is relatively similar for all sites along the climatic gradient. The effect of warmer climate conditions on the vegetation development, such as a longer and warmer growing season were not tested in this scenario, because the climate conditions in ArcVeg are stochastically determined based on the region (not varied), rather than observed air temperature data as used in WIT. It can however be expected that faster plant growth have an effect on size and distribution of nonsorted circles and may be the leading cause for ecosystem alterations. Deeper active layers and dryer conditions, a side effect of warming conditions, both lead to an additional decrease in the number density of nonsorted circles in the system and a likely increase in the vegetated cover.

[27] The active layer depth before onset of freezing is a direct effect of local summer climate conditions and has a strong effect on pattern formation and an indirect effect on soil wetness [*Hinzman et al.*, 2005]. The effect of deeper active layer depth is caused by the longer freezing period (water movement) experienced with a deeper active layer. The result, as shown, is that the model simulates larger and fewer features with deeper active layer depths. The extended period of water migration assures less ice accumulation in the vegetated areas and therefore faster biomass accumulation.

[28] Soil texture plays an important role during the freezing process [*Vliet-Lanoe*, 1985]. Soil texture and secondary soil structure determines the soil freezing characteristics curve and the ability for the soil to transport liquid water in a freezing soil [*Lundin*, 1990]. Moisture migration due to a temperature gradient occurs when the soil is partially frozen. The hydraulic conductivity at that time depends on the liquid water content and the effective porosity of the frozen soil. The liquid water content depends on the soil temperature and the soil particle distribution. At below freezing temperatures the liquid water content reduces and the suction in the soil increases. For a sandy soil the liquid water content decreases faster with increasing suction compared with finer grained soils [*French*, 2007]. Clay on the other hand harbors a large amount of liquid water at relatively low temperatures (high level of suction). However, in clay the hydraulic conductivity is much smaller, which limits the liquid water movement. The results show therefore a pattern with more and smaller features.

5. Conclusions and Future Research

[29] We have analyzed the relation between plant biomass and soil surface insulation expressed using R-value. We determined that there is a complex relation between mea-

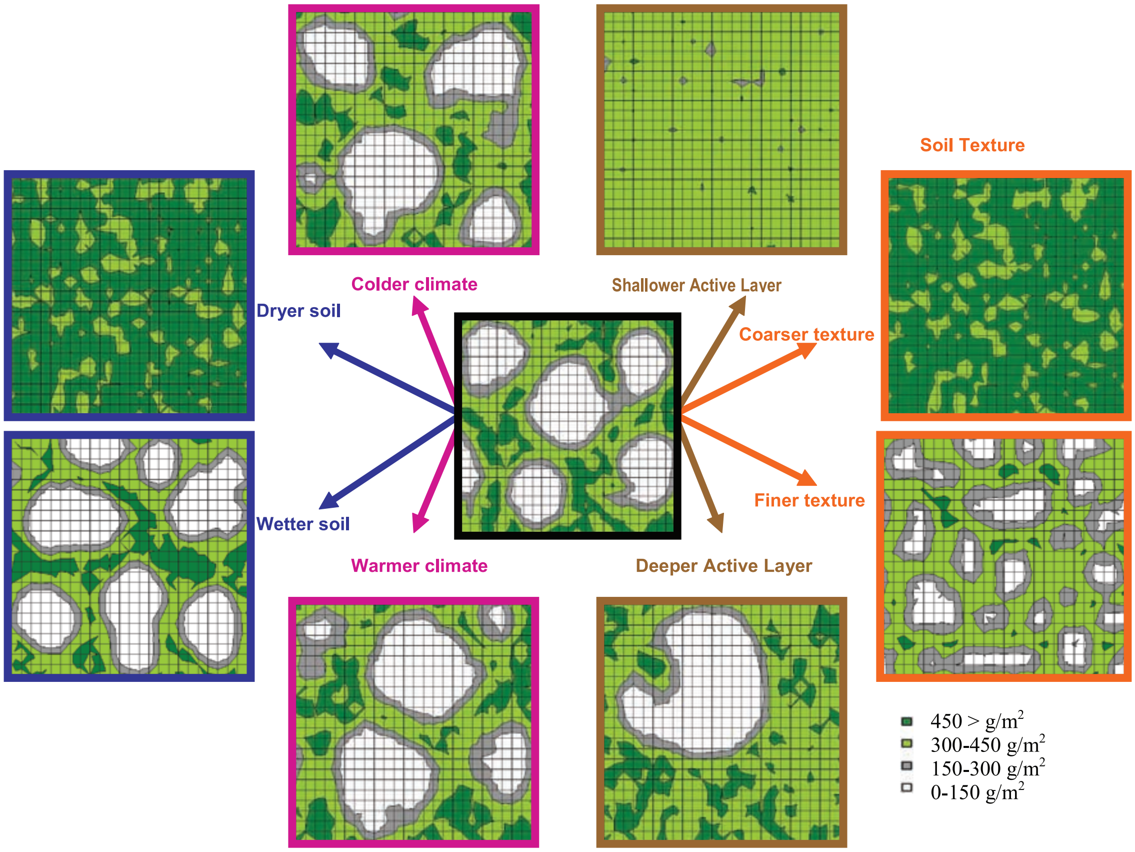

Figure 5. Sensitivity analysis of variation of parameters such as soil moisture, air temperature, active layer depth and soil texture. The colors reflect biomass after 861 years of vegetation development. The size of the domain is the same as in Figure 4.

sured R-values of the soil surface and biomass. Mosses and snow are generally believed to be very important in determining surface insulation. We found that these two predictors alone do not adequately describe winter soil surface insulation along the NAAT.

[30] WIT-ArcVeg is the first model that shows nonsorted circle pattern formation from random vegetation development through solving coupled heat and moisture transport with phase change in the active layer of the Arctic Tundra.

[31] Multiple scenario simulations with the model demonstrate the effects of environmental conditions on pattern formation. Water availability is very important for pattern formation. Water availability is affected by soil wetness, depth and texture of the active layer. Active layer depth also influences the duration of the freezing period and affects the size of the nonsorted circle features that form and stabilize. Change in climatic conditions on the freezing process show no effect on the pattern formation, which implies that the cooling rate during the freezing period is very similar along all the sites of the NAAT.

[32] Further analysis on the effects of vegetation on insulation and water movement are needed to better quantify the effect of each plant type on the stability of the nonsorted circle system. In particular we want to research the tipping point of nonsorted circle collapse toward complete vegetative cover, which has a major effect on larger scale processes of albedo, permafrost dynamics and carbon storage.

[33] **Acknowledgments.** Financial support for this research from the Arctic Regions Supercomputing Center of the University of Alaska Fairbanks is duly acknowledged. Field data used in this research were made available through a grant by the National Science Foundation OPP-0120736. The authors wish to acknowledge the personal support provided by Frank Williams, Director, and Greg Newby, Chief Scientist, the Arctic Regions Supercomputing Center, UAF.

References

Boike, J., O. Ippisch, and K. Roth (2002), Thermal and hydrological dynamics of a mud boil—Any clues about its formation?, *J. Geocryol. Glaciol.*, *24*(5), 538–543.

Chapin, F. S., III, et al. (2005), Role of terrestrial ecosystem changes in arctic summer warming, *Science*, *310*, 657–660.

Daanen, R. P. (2004), Modeling liquid water flow in snow, Ph.D. thesis, Univ. of Minn., Minneapolis.

Daanen, R. P., D. Misra, and H. E. Epstein (2007), Active-layer hydrology in nonsorted circle ecosystems of the Arctic Tundra, *Vadose Zone J.*, *6*, 694–704, doi:10.2136/vzj2006.0173.

Epstein, H. E., M. D. Walker, F. S. Chapin III, and A. M. Starfield (2000), A transient, nutrient based model of arctic plant community response to climate warming, *Ecol. Appl.*, *10*, 824–841.

Epstein, H. E., F. S. Chapin III, M. D. Walker, and A. M. Starfield (2001), Analysing functional type concept in arctic plants using a dynamic vegetation model, *Oikos*, *95*, 239–252.

Fowler, A. C., and W. B. Krantz (1994), A generalized secondary frost heave model, *SIAM J. Appl. Math.*, *54*(6), 1650–1675.

French, H. M. (2007), *The Periglacial Environment*, Wiley, Chichester.

Hinzman, L. D., et al. (2005), Evidence and implications of recent climate change in northern Alaska and other arctic regions, *Clim. Change*, *72*(3), 251–298.

Ippisch, O. (2003), Coupled transport in natural porous media, Ph.D. thesis, Univ. of Heidelberg, Heidelberg, Germany.

Jia, G. J., H. E. Epstein, and D. A. Walker (2003), Greening of the Alaskan Arctic over the past two decades, *Geophys. Res. Lett.*, *30*(20), 2067, doi:10.1029/2003GL018268.

Jonasson, S., and T. V. Callaghan (1992), Root mechanical-properties related to disturbed and stressed habitats in the Arctic, *New Phytol.*, *122*, 179–186.

Kade, A., V. E. Romanovsky, and D. A. Walker (2006), The N-factor of nonsorted circles along a climate gradient in Arctic Alaska, *Permafrost Periglac, Processes*, *17*(4), 279–289.

Lundin, L. C. (1990), Hydraulic properties in an operational model of frozen soil, *J. Hydrol. Amsterdam*, *118*(1–4), 289–310.

Maxwell, B. (1992), *Arctic Climate: Potential for Change Under Global Warming*, pp. 11–34, Academic, San Diego, Calif.

Miller, R. D. (1980), *Freezing Phenomena in Soil: Applications of Soil Physics*, pp. 254–299, Academic, San Diego, Calif.

Mitchell, J. K. (1993), *Fundamentals of Soil Behavior*, 543 pp., John Wiley, New York.

Myneni, R. B., C. D. Keeling, C. J. Tucker, G. Asar, and R. R. Nemani (1997), Increased plant growth in the northern high latitudes from 1981 to 1991, *Nature*, *386*, 698–702.

Nicolsky, D. J., G. S. Tipenko, and V. E. Romanovsky (2004), A coupled thermo-mechanical model of the differential frost heave, *Eos Trans. AGU, Fall Meet. Suppl.*, *85*(47), Abstract C13-B-0282.

Peterson, R. A., and W. B. Krantz (2003), A mechanism for differential frost heave and its implications for patterned ground formation, *J. Glaciol.*, *49*, 69–80.

Raynolds, M. K., D. A. Walker, C. A. Munger, C. M. Vonlanthen, and A. N. Kade (2008), A map analysis of patterned-ground along a North American Arctic Transect, *J. Geophys. Res.*, *113*, G03S03, doi:10.1029/2007JG000512.

Shaver, G. R., M. S. Bret-Harte, H. M. Jones, L. Johnstone, L. Gough, J. A. Laundre, and F. S.I. Chapin (2001), Species composition interacts with fertilizer to control long-term change in tundra productivity, *Ecology*, *82*, 3163–3181.

Sturm, M., T. Douglas, C. Racine, and G. E. Liston (2005), Changing snow and shrub conditions affect albedo with global implications, *J. Geophys. Res.*, *110*, G01004, doi:10.1029/2005JG000013.

Tape, K., M. Sturm, and C. Racine (2006), The evidence for shrub expansion in northern Alaska and the pan-Arctic, *Global Change Biol.*, *12*, 686–702.

van Genuchten, T. M. (1980), A closed form equation for predicting the hydraulic conductivity of unsaturated soil, *Soil Sci. Soc. Am. J.*, *44*, 892–898.

Vliet-Lanoe, B. V. (1985), *Frost Effect in Soils: Soils and Quaternary Landscape Evolution*, pp. 117–158, John Wiley, Hoboken, N. J.

Vliet-Lanoe, B. V. (1991), Differential frost heave, load casting and convection: Converging mechanisms; a discussion of the origin of cryoturbations, *Permafrost Periglac, Processes*, *2*, 123–139.

Walker, D. A., et al. (2004), Frost-boil ecosystems: Complex interactions between landforms, soils, vegetation, and climate, *Permafrost Periglac, Processes*, *15*, 171–188.

Walker, D. A., et al. (2008), Arctic patterned-ground ecosystems: A synthesis of field studies and models along a North American Arctic Transect, *J. Geophys. Res.*, *113*, G03S01, doi:10.1029/2007JG000504.

Walker, M., et al. (2006), Plant community response to experimental warming across the tundra biome, *Proc. Natl. Acad. Sci. U. S. A.*, 1342–1346.

Walsh, J. E. (1993), The elusive Arctic warming, *Nature*, *361*(6410), 300–301.

Washburn, A. L. (1956), Classification of patterned ground and review of suggested origins, *Geol. Soc. Am. Bull.*, *67*, 823–866.

Washburn, A. L. (1997), *Plugs and plug circles; a basic form of patterned ground, Cornwallis Island, Arctic Canada; origin and implications*, Quat, Res. Cent., Univ. of Wash, Seattle.

R. P. Daanen and V. Romanovsky, Permafrost Laboratory, Geophysical Institute, University of Alaska Fairbanks, Fairbanks, AK 99775, USA. (ffrd@uaf.edu; ffver@uaf.edu)

H. Epstein, Department of Environmental Sciences, University of Virginia, Charlottesville, VA 22904, USA. (hee2b@virginia.edu)

D. Misra, Department of Mining and Geological Engineering, College of Engineering and Mines, University of Alaska Fairbanks, Fairbanks, AK 99775, USA. (debu.misra@uaf.edu)

D. Walker, Department of Biology and Wildlife, University of Alaska Fairbanks, Fairbanks, AK 99775, USA. (ffdaw@uaf.edu)